

Near-infrared silicon quantum dots metal-oxide-semiconductor field-effect transistor photodetector

Jia-Min Shieh, Wen-Chien Yu, Jung Y. Huang, Chao-Kei Wang, Bau-Tong Dai, Huang-Yan Jhan, Chih-Wei Hsu, Hao-Chung Kuo, Fu-Liang Yang, and Ci-Ling Pan

Citation: *Applied Physics Letters* **94**, 241108 (2009); doi: 10.1063/1.3156806

View online: <http://dx.doi.org/10.1063/1.3156806>

View Table of Contents: <http://scitation.aip.org/content/aip/journal/apl/94/24?ver=pdfcov>

Published by the *AIP Publishing*

Articles you may be interested in

Escape dynamics of a few electrons in a single-electron ratchet using silicon nanowire metal-oxide-semiconductor field-effect transistor

Appl. Phys. Lett. **93**, 222103 (2008); 10.1063/1.3028649

Enhanced photoresponse of a metal-oxide-semiconductor photodetector with silicon nanocrystals embedded in the oxide layer

Appl. Phys. Lett. **90**, 051105 (2007); 10.1063/1.2450653

Quantum transport in a nanosize double-gate metal-oxide-semiconductor field-effect transistor

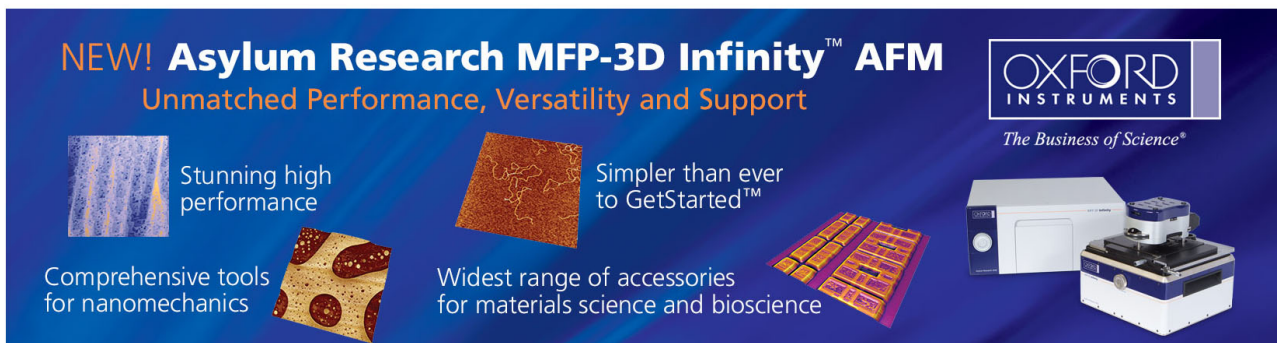
J. Appl. Phys. **96**, 2305 (2004); 10.1063/1.1767619

Coulomb oscillations based on band-to-band tunneling in a degenerately doped silicon metal-oxide-semiconductor field-effect transistor

Appl. Phys. Lett. **84**, 3178 (2004); 10.1063/1.1707217

Ge/Si quantum-dot metal-oxide-semiconductor field-effect transistor

Appl. Phys. Lett. **80**, 4783 (2002); 10.1063/1.1488688

The advertisement features a dark blue background with a grid of images showing various AFM scans and the physical instrument. The text is in white and orange. The Oxford Instruments logo is in the top right corner.

NEW! Asylum Research MFP-3D Infinity™ AFM
Unmatched Performance, Versatility and Support

OXFORD INSTRUMENTS
The Business of Science®

Stunning high performance

Simpler than ever to GetStarted™

Comprehensive tools for nanomechanics

Widest range of accessories for materials science and bioscience

Near-infrared silicon quantum dots metal-oxide-semiconductor field-effect transistor photodetector

Jia-Min Shieh,^{1,2,a)} Wen-Chien Yu,¹ Jung Y. Huang,² Chao-Kei Wang,¹ Bau-Tong Dai,¹ Huang-Yan Jhan,² Chih-Wei Hsu,² Hao-Chung Kuo,² Fu-Liang Yang,¹ and Ci-Ling Pan^{2,3}

¹National Nano Device Laboratories, No. 26 Prosperity Road 1, Hsinchu 30078, Taiwan

²Department of Photonics and Institute of Electro-Optical Engineering, National Chiao Tung University, 1001 Ta Hsueh Road, Hsinchu 30010, Taiwan

³Department of Physics and Institute of Photonics Technologies, National Tsing Hua University, 101 Section 2, Kuang-Fu Road, Hsinchu 30013, Taiwan

(Received 13 February 2009; accepted 1 June 2009; published online 17 June 2009)

A fully silicon-based metal-oxide-semiconductor field-effect transistor is demonstrated for the detection of near-infrared light. Si nanocrystals (nc-Si) are synthesized in the nanopore channels of mesoporous silica (MS) inserted between two oxide layers to form a complete gate structure of polycrystalline Si/SiO₂/nc-Si-in-MS/SiO₂ with a polycrystalline Si electrode. Illuminating the gate with near-infrared light, a photoresponsivity as high as 2.8 A/W at 1.55 μm can be achieved. The improved photoresponsivity is attributed to from optical transitions via interface states and a current amplification mechanism of the device. © 2009 American Institute of Physics.

[DOI: 10.1063/1.3156806]

Silicon (Si) optoelectronics is one of the highly desired developments in photonics owing to its full compatibility with the silicon microelectronics industry. Unfortunately, bulk Si crystal is unsuited for applications as light source and detector in the telecommunication wavelength region ($1.3 \mu\text{m} < \lambda < 1.6 \mu\text{m}$) because Si crystal does not absorb long-wavelength photons efficiently. Recently, enabling by nanotechnology the concept of functionality by design has attracted significant interest of researchers. Based on the concept, “architectural photonics” has been developed to yield improved functionality by tailoring the device geometry or the structure of material used.

Optoelectronic properties of Si nanocrystals (nc-Si) are quite different from their bulk counterpart. Although silicon belongs to an indirect bandgap semiconductor, nc-Si embedded in SiO₂ exhibit visible photoluminescence with high efficiency.¹ In our previous study, we found that nc-Si synthesized in the nanopore channels of mesoporous silica (nc-Si-MS) can yield an improved optoelectronic response over the visible spectrum region.² High-speed Si optical modulator with a metal-oxide-semiconductor (MOS) structure³ had been proposed as a core component of Si photonics. Along this thinking, Si-based near-infrared (NIR) detector is also highly desired. Si-based NIR detection had been demonstrated with a porous-Si Schottky barrier photodetector (PD).⁴ However, due to its non-thin-film-based technology the porous-Si Schottky barrier device cannot integrate with other devices to form an optoelectronic system.

Recently, a three-terminal MOS field-effect transistor (MOSFET) PD with Ge gate⁵ as the NIR light absorption layer had been reported. The photoexcited carriers in the Ge gate, generated by 1.55 μm NIR light absorption, form a net gate current due to band bending under gate bias. The gate current charges the gate structure and results in an accumu-

lation of electrons and holes at either side of the gate insulator. A carrier density increase in the channel layer then raises the gate current at the drain terminal.

In this letter, we report an nc-Si/MS based three-terminal MOSFET, which exhibits an improved NIR optoelectronic response. The operational principle of our nc-Si/MS based three-terminal MOSFET PD is different from the scenario depicting above.⁵ We show that the nc-Si/MS can be employed to surpass the limit of the fundamental bandgap of bulk silicon crystal. The formation of nc-Si in mesoporous silica modifies the surface bonding structure of the pore channels,⁶ inducing enhanced optoelectronic response in the material.²

We first characterized the optoelectronic response of a nc-Si/MS layer by fabricating a two-terminal MOS on a *p*-type Si substrate with the structure of indium tin oxide (ITO) electrode/(nc-Si/MS)/*p*-Si.² The resulting photoresponsivity is presented in Fig. 1 with open symbols. For comparison, the photoresponsivity of a *pn* diode (namely, ITO/*n*-Si/*p*-Si) is also included (the dashed line). The photoresponsivity of this reference device reversely biased at 5 V increases with wavelength from 300 to 900 nm. The spectral response of the device is restricted to below 1.1 μm from the limit of silicon fundamental bandgap.

The measured photoresponsivity of the ITO/(nc-Si/MS)/*p*-Si PD at the same bias voltage lies in the range of 0.4–1.0 A/W from 320 to 900 nm, significantly higher than those of the reference Si PD. In the visible spectral region, our ITO/(nc-Si/MS)/*p*-Si MOS PD exhibits three resonances at 420, 560, and 770 nm with peak values of 0.4, 0.7, and 0.9 A/W, respectively. The improvement was attributed to a transistorlike gain mechanism.² At a reverse bias, the primary photoexcited carriers generated in the Si quantum dots (QDs) of the nc-Si/MS layer can be amplified with electron injection process from the inversion layer through the MS dielectric to the ITO electrode. An optoelectronic conversion efficiency as high as 800% had been

^{a)}Author to whom correspondence should be addressed. Electronic addresses: jmshieh@ndl.org.tw or jmshieh@faculty.nctu.edu.tw.

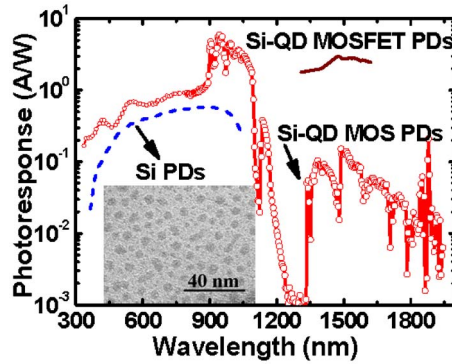


FIG. 1. (Color online) Photoreponse of a two-terminal photo-detector with ITO electrode/(nc-Si-in-MS)/*p*-Si MOS structure (the curve with symbols) and a *pn* diode (ITO/*n*-Si/*p*-Si) (the dashed line). The inset shows the cross-sectional TEM image of the nc-Si-in-MS film with high density of nc-Si. The solid curve indicates the photoreponse spectrum of a three-terminal MOSFET PD with a gate structure of poly-Si/SiO₂/(nc-Si-in-MS)/SiO₂.

achieved.² The appearance of resonances in the visible spectral region shown in Fig. 1 suggests that the optical response could be resonantly enhanced with the electronic structure of nc-Si/MS. The photoreponse peaks at 420 and 560 nm correspond to a resonant energy of 3.0 and 2.2 eV, respectively.^{2,7,8} The energy difference of the two resonances is 0.8 eV, suggesting an intraband transition^{9–11} at 1.55 μm to be allowed.¹² The gap existing from 1.2~1.3 μm in the photoreponse spectrum of our ITO/(nc-Si/MS)/*p*-Si MOS PD indicates that the observed NIR optoelectronic response longer than 1.3 μm could not be due to transitions via band-tail states.¹³ The measured photoresponsivity of our ITO/(nc-Si/MS)/*p*-Si MOS PD from 1.3 to 1.9 μm is also higher than that of other nc-Si MOS device by eight orders of magnitude.¹²

The schematic energy-level diagram shown in Fig. 2(a) was drawn to facilitate the illustration of the optical transitions involved in nc-Si/MS. The absorption process of incoming visible photons can take place directly inside the embedded Si QDs or via interface states between QDs and mesoporous silica matrix; while for the NIR photons, transitions via nc-Si/MS interface states dominate.^{2,7,8,10}

We fabricated a fully Si-based NIR MOSFET PD (Ref. 5) with a thin-film transistor process.¹⁴ The device

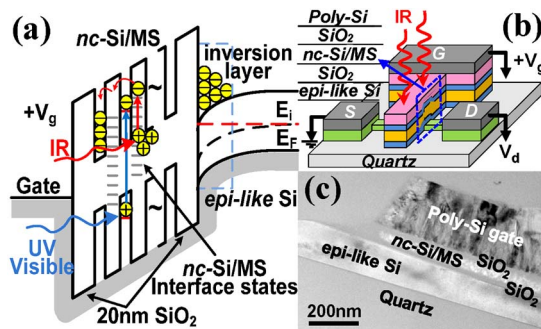


FIG. 2. (Color online) (a) Energy-level diagram used to illustrate the optical transitions involved in nc-Si/MS. (b) Schematic of the MOSFET detector. (c) The cross-sectional TEM image of a MOSFET device with a gate structure of poly-Si/SiO₂/nc-Si-in-MS/SiO₂. The gate dielectric stack is comprised of a 55 nm thick nc-Si/MS film sandwiched between 20 nm thick SiO₂ buffer layers.

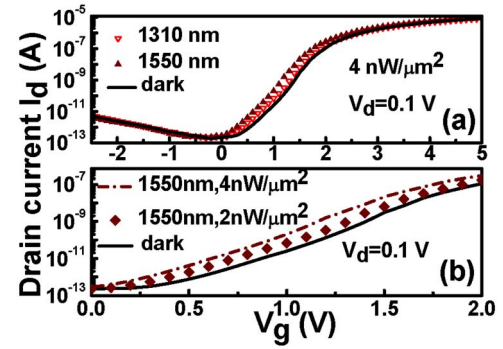


FIG. 3. (Color online) (a) The I_d - V_g characteristics of the MOSFET PD in the dark and illuminated by a light beam at 1310 and 1550 nm, respectively. (b) The I_d - V_g characteristics of the MOSFET PD illuminated with 2 and 4 $\text{nW}/\mu\text{m}^2$ at 1550 nm.

comprises a gate structure of polycrystalline Si/SiO₂/nc-Si-in-MS/SiO₂, as depicted in Figs. 2(b) and 2(c), possessing a 6 μm long channel with a width of 25 μm made from an epilike Si layer on a quartz substrate.¹⁴ The gate dielectric structure consists of a 55 nm thick nc-Si/MS film sandwiched between two 20 nm thick oxide buffer layers. The source and drain regions of the MOSFET were doped with PH₃ ($5.0 \times 10^{15} \text{ cm}^{-2}$ at 25 keV) and then activated by a 532 nm cw laser with an averaged power of 2.2–2.8 W.¹⁴

The MOSFET detector was characterized by measuring the curves of drain current (I_d)-gate voltage (V_g) and drain current (I_d)-drain voltage (V_d). The I_d - V_g characteristics of the MOSFET device with the gate being kept in the dark or illuminated with NIR light at 1310 and 1550 nm are presented in Fig. 3(a). Hole trapping in the illuminated gate produces a built-in potential that adds to an external bias (V_g) to generate a negative shift (ΔV_{th}) of the threshold voltage (V_{th}).^{2,15} Therefore, the device with illuminated gate generates a higher drain current. The threshold voltage shift depends on the density of trapped holes [see Fig. 3(b)]. As the device is irradiated with 1.55 μm light, ΔV_{th} becomes larger than that with 1.31 μm light, implying that 1.55 μm photons can more efficiently generate photoexcited carriers at the interface states of nc-Si/MS.¹³ In the off-state with negative V_g , the photocurrent generated by NIR light is very low due to a very low leakage experienced by the drain current at the reversely biased drain-to-channel junction.

The I_d - V_d characteristics of the MOSFET PD operated at various gate bias voltages with the unexposed gate structure or illuminated with 1310 and 1550 nm light, respectively, at an irradiance of 4 $\text{nW}/\mu\text{m}^2$ are presented in Fig. 4(a). The corresponding photoresponsivity is shown in Fig. 4(b). The wavelength ($1.3 \mu\text{m} < \lambda < 1.6 \mu\text{m}$) dependence of the photoresponsivity is plotted in Fig. 1 with a solid curve, revealing the photoreponse of the MOSFET PD at 1550 nm to be 2.8 A/W at $V_g = 1.6 \text{ V}$ and $V_d = 3 \text{ V}$. The high photoresponsivity can be attributed to a current gain from the transistor mechanism.

An energy-level model was proposed to illustrate the experimental observations reported above. Without illumination, the device behaves like a normal MOSFET. When the gate voltage ($+V_g$) is higher than the threshold voltage, a significant number of electrons can accumulate at the interface between the gate structure and the epilike Si channel to

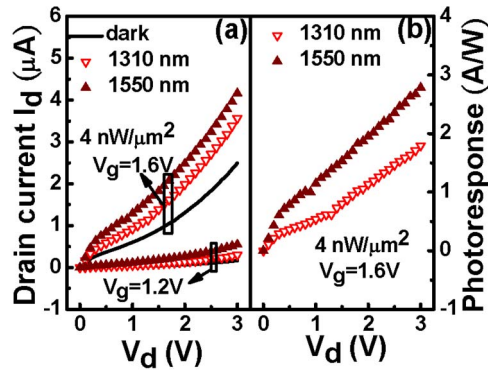


FIG. 4. (Color online) (a) The I_d - V_d characteristics of the MOSFET PD operated with two different gate bias voltages. The device was kept in the dark or its gate region was illuminated by 1310 and 1550 nm light, respectively, with an irradiance of $4 \text{ nW}/\mu\text{m}^2$. (b) The corresponding photore-sponsivity of the device with a gate bias voltage of 1.6V is plotted as a function of V_d .

form an n -type inversion layer. As a result, the gate voltage induces a drain current. When the energy of an incident photon matches a difference between an occupied electronic state to an empty excited state, a strong absorption occurs. The lowest energy of photons can be absorbed by a bonding structure located at an interface is the energy gap between the highest occupied molecular orbital and the lowest unoccupied orbital.⁸ The most likely interfacial states are the bonding orbitals of Si-O.² Under an applied electric field, the photoexcited electrons can tunnel to the interface of the upper blocking oxide layer and the nc-Si/MS layer.² The holes, however, are trapped at the interface states.^{2,15} The immobilized positive charges together with accumulated electrons at the oxide/nc-Si/MS interface form a net polarization in the nc-Si/MS layer as illustrated in Fig. 2(a). This polarization enhances the influence of the gate voltage ($+V_g$) and increases the channel conductance, which causes more electrons to flow from the source to the positively biased drain terminal.

In the nc-Si/MS MOSFET PD, a very small increase in the gate current (~ 22 – 79 pA at $V_g=0$ – 3 V and $V_d=3 \text{ V}$, data not shown) under illumination ensures the MOSFET to operate in the “voltage-controlled-current” mode. The optical absorption by silicon nanocrystals is extremely fast in the order of picoseconds.¹⁶ Therefore, the gate response time τ is mainly limited by the transport time of the photoexcited carriers. For a gate structure with 55 nm thick (d) nc-Si/MS, we estimated the response time to be about 1 ns by using $\tau=d^2/(V\mu)$,¹⁷ where V is the applied bias and μ is the effective mobility of nc-Si/MS. The effective mobility of our nc-Si/MS was determined to be $10^{-2} \text{ cm}^2/\text{V s}$ from the observed photoreponse time (10 ns) on a 220 nm thick

nc-Si/MS MOS PD.² Note that this value is about one order of magnitude higher than the reported result with a thin film of Si nanoparticles.¹⁷ For the nc-Si/MS three-terminal MOSFET PD, a device response time of 2 ns was achieved, which is mainly limited by the carrier transport time of the micrometers-long epi-Si channel used.⁵

In summary, we had developed an nc-Si MOSFET PD to surpass the limitation of the fundamental bandgap of bulk silicon crystal. The absorption in the NIR region of $1.3 \mu\text{m} < \lambda < 1.6 \mu\text{m}$ can occur via transitions in nc-Si/MS interface states. The photocarriers generated by NIR photons in the nc-Si/MS gate layer enhance the influence of gate bias and result in an increase in the electron density in the inversion layer of the channel. The phototransistor mechanism of our device further amplifies the photore-sponsivity at $1.55 \mu\text{m}$ to 2.8 A/W .

The authors would like to thank the National Science Council of the Republic of China, Taiwan for partially supporting this research.

¹Z. H. Lu, D. J. Lockwood, and J. M. Baribeau, *Nature (London)* **378**, 258 (1995).

²J. M. Shieh, Y. F. Lai, W. X. Ni, H. C. Kuo, C. Y. Fang, J. Y. Huang, and C. L. Pan, *Appl. Phys. Lett.* **90**, 051105 (2007).

³A. Liu, R. Jones, L. Liao, D. Samara-Rublo, D. Rubin, O. Cohen, R. Nicolaescu, and M. Pannicia, *Nature (London)* **427**, 615 (2004).

⁴M. K. Lee, C. H. Chu, Y. H. Wang, and S. M. Sze, *Opt. Lett.* **26**, 160 (2001).

⁵A. K. Okyay, A. J. Pethe, D. Kuzum, S. Latif, D. A. Miller, and K. C. Saraswat, *Opt. Lett.* **32**, 2022 (2007).

⁶A. T. Cho, J. M. Shieh, J. Shieh, Y. F. Lai, B. T. Dai, F. M. Pan, H. C. Kuo, Y. C. Lin, K. J. Chao, and P. H. Liu, *Electrochem. Solid-State Lett.* **8**, G143 (2005).

⁷M. V. Wolkin, J. Jorne, P. M. Fauchet, G. Allan, and C. Delerue, *Phys. Rev. Lett.* **82**, 197 (1999).

⁸A. Puzder, A. J. Williamson, J. C. Grossman, and G. Galli, *Phys. Rev. Lett.* **88**, 097401 (2002).

⁹P. Boucaud, V. Le Thanh, S. Sauvage, D. Débarre, and D. Bouchier, *Appl. Phys. Lett.* **74**, 401 (1999).

¹⁰J. S. de Sousa, J. P. Leburton, V. N. Freire, and E. F. da Silva, Jr., *Appl. Phys. Lett.* **87**, 031913 (2005).

¹¹C.-H. Lin, C.-Y. Yu, C.-Y. Peng, W. S. Ho, and C. W. Liu, *J. Appl. Phys.* **101**, 033117 (2007).

¹²S. M. Hossain, A. Anopchenko, S. Prezioso, L. Ferraioli, L. Pavesi, G. Pucker, P. Bellutti, S. Binetti, and M. Acciarri, *J. Appl. Phys.* **104**, 074917 (2008).

¹³A. U. Savchouk, S. Ostapenko, G. Nowak, J. Lagowski, and L. Jastrzebski, *Appl. Phys. Lett.* **67**, 82 (1995).

¹⁴J. M. Shieh, C. Chen, Y. T. Lin, and C. L. Pan, *Appl. Phys. Lett.* **92**, 063503 (2008).

¹⁵S. H. Choi and R. G. Elliman, *Appl. Phys. Lett.* **74**, 3987 (1999).

¹⁶E. Lioudakis, A. Othonos, and A. G. Nassiopoulou, *Appl. Phys. Lett.* **90**, 171103 (2007).

¹⁷O. M. Nayfeh, S. Rao, A. Smith, J. Therrien, and M. H. Nayfeh, *IEEE Photonics Technol. Lett.* **16**, 1927 (2004).